Numerical Investigation of Radiative Heat Transfer in a Particulate Medium Using FTn Finite Volume Method

Moghadassian, Behnam; Jafari, Mohammad ; Hafezisefat, Parinaz ; M. Hosseini, S. Mojtaba; Rezaniakolaei, Alireza

Published in:
Energy Procedia

DOI (link to publication from Publisher):
10.1016/j.egypro.2019.01.566

Publication date:
2019

Document Version
Publisher's PDF, also known as Version of record

Available online at www.sciencedirect.com

ScienceDirect

Energy Procedia 158 (2019) 5692–5698

Energy Procedia

www.elsevier.com/locate/procedia

10th International Conference on Applied Energy (ICAE2018), 22-25 August 2018, Hong Kong, China

Numerical Investigation of Radiative Heat Transfer in a Particulate Medium Using FTn Finite Volume Method

Behnam Moghadassian[a,*], Mohammad Jafari[a], Parinaz Hafezisefat[b], Mojtaba Mirhosseini[c], Alireza Rezania[c]

[a]*Department of Aerospace Engineering, Iowa State University, Ames, Iowa, USA*
[b]*Department of Mechancial Engineering, Iowa State University, Ames, Iowa, USA*
[c]*Department of Energy Technology, Aalborg University, Pontoppidanstraede 111, 9220 Aalborg East, Denmark*

Abstract

Radiative heat transfer in participating medium finds applications in high temperature systems where the medium is not perfectly transparent. Examples are combustion chambers and layers of Earth's atmosphere. Presence of tiny particles (ranging from 500 nanometers to 10 micrometers in diameter) in a medium strongly affects the radiative heat transfer. The governing equations for solving the heat transfer in the medium are discretized using FT*n* finite volume method. The major step in simulating the radiative heat transfer in a particulate medium is finding the scattering phase function. The original Mie theory (without any approximation) is used to calculate scattering phase functions. Non-orthogonal mesh is applied to discretize the non-orthogonal computational domain. The intensities at cell faces are found by relating them to nodal values through the high resolution CLAM scheme. Cases of scattering in media with dielectric particles and absorbing particles are considered. Also, the influences of the particle density on the dimensionless radiative heat flux and direction-integrated intensity are studied.

Keywords: Radiative heat transfer; Scattering phase function; FT*n* finite volume method; Particulate media; Nano particles

1. Introduction

In various high temperature engineering applications, radiation is either the dominant mode of heat transfer or at least its contribution in overall heat transfer cannot be neglected. In many cases in both nature and science, there are

* Corresponding author. Tel.: +1-979-492-5978;
E-mail address: behmogh@iastate.edu

10.1016/j.egypro.2019.01.566

particles of different sizes (usually in the order of micro- and nano-sizes) floating in the participating media that make the scattering phenomena more complicated. Such media is known as particulate media. Trivic et al. [1] considered Mie scattering in the square and cubic enclosures. They successfully coupled the finite volume method (FVM) with Mie theory to perform a numerical study of the effect of anisotropic scattering on the radiative heat transfer. Khademi Moghadam et al. [2] presented the solution for transient radiative heat transfer in irregular geometries. They discretized the transient radiative transfer equation (TRTE) by finite volume method (FVM) and compared Mie theory to isotropic approximation.

So far, various numerical methods have been proposed for solving radiative transfer equation (RTE). These methods can be classified into two general groups. One group includes methods based on the RTE discretization such as discrete ordinate method (DOM) [3], finite-volume method (FVM) [4, 5], finite element method (FEM) [6, 7]. The other encompasses the methods based on ray-tracing technique such as Monte Carlo method [8] and zonal method [9]. In addition to be consistent with other numerical techniques used in determining the flow and temperature fields, the methods of the first category have other merits such as being easily programmable, fairly accurate and computationally cheap. A comprehensive review on the development of various solution methods of RTE can be found in the books of Modest [10] and Siegel and Howell [11]. Finite volume and finite element methods have been widely used and proved to be effective, not only for radiative heat transfer problems but also in many numerical simulations of the fluid flow and heat transfer. FVM has been used successfully in problems of porous media [12], cylindrical geometries [13], combustion applications [14], irregular geometries [15], and conjugate heat transfer [16]. Kim and Huh [17] proposed FT*n* FVM specifically for radiative heat transfer problems. They utilized a new angular discretization and demonstrated that the ray effects become less by using this angular grid in comparison with classical FVM. FT*n* FVM was successfully used in radiative problem in inhomogeneous media and the irregular geometries of the combustion chambers [18].

The goal of this study is to assess the effects of Mie scattering in radiative heat transfer in an irregular geometry. The numerical solution consists the coupling of Mie theory and FT*n* FVM with CLAM scheme and non-orthogonal grid. Different cases of the forward, backward and isotropic scattering as well as scattering in media with real and complex index of refraction are studied. Moreover, the effect of particle sizes on the radiation heat transfer is investigated.

Nomenclature

a	coefficients in FVM equation
a_p	radius of spherical particles
G	direction-integrated intensity [10]
I	radiation intensity [10]
L	length
n	refractive index
n	number of divisions of polar angle in FT*n* FVM
n	unit vector normal to control surface
q	radiative heat flux vector [10]
Q_{ext}	extinction efficiency factor [10]
Q_{sca}	scattering efficiency factor [10]
r	spatial position vector
s	unit vector in the direction of intensity
x, y, z	Cartesian coordinates
x_p	particle size parameter

Greek symbols

β	extinction coefficient [10]
ε	wall emissivity
σ	Stefan-Boltzmann constant
λ	wavelength
σ_s	scattering coefficient
Φ	scattering phase function
Ψ	scattering angle [10]
ω	single scattering albedo ($=\sigma_s/\beta$)
Ω	solid angle

2. Mathematical formulation for RTE solver

The radiative transfer equation in a grey emitting, absorbing and scattering media at any position, *r*, along a path, *s*, is given by:

$$\frac{dI(\mathbf{r},\mathbf{s})}{ds} = -\beta I(\mathbf{r},\mathbf{s}) + S(\mathbf{r},\mathbf{s}) \tag{1}$$

where the source function can be defined as:

$$S(\mathbf{r},\mathbf{s}) = -\kappa I_b(\mathbf{r}) + \frac{\sigma_s}{4\pi}\int I(\mathbf{r},\mathbf{s})\Phi(\mathbf{s},\mathbf{s}')d\Omega \tag{2}$$

The boundary condition for a diffusely emitting and reflecting wall can be written as follows:

$$I(\mathbf{r}_w,\mathbf{s}) = \varepsilon_w I_b(\mathbf{r}_w,\mathbf{s}) + \frac{1-\varepsilon}{\pi}\int_{\mathbf{n}_w\cdot\mathbf{s}'<0} I(\mathbf{r}_w,\mathbf{s}')|\mathbf{n}_w\cdot\mathbf{s}'|d\Omega' \tag{3}$$

The angular discretization for popular FVM and FT*n* FVM is shown in Figs. 1a and 1b, respectively. For popular FVM the angular domain is uniformly subdivided into N_θ and N_ϕ in polar and azimuthal angles, respectively. As it can be seen, the control angles do not have the same size (they are smaller near the poles). But for FT*n* FVM the polar angle is distributed into *n* uniform subdomains where *n* is an even number. The azimuthal angle is then divided into the number of sequence of 4, 8, …, 12, 2*n*, …, 12, 8, 4 in each level of polar angle. They have almost the same size with the aspect ratio of unity. The total number of control angles is $N_s=n(n+2)$.
The discretization procedure of RTE is according to that of Chai et al. [5] and is not repeated here. Integrating the RTE (Eq. (1)) over a 2D non-orthogonal control volume (Fig. 1c) and over a control angle of FT*n* FVM (Fig. 1b), the final discretized equation can be derived as [5]:

$$a_P^l I_P^l = a_W^l I_W^l + a_E^l I_E^l + a_N^l I_N^l + a_S^l I_S^l + b^l \tag{4}$$

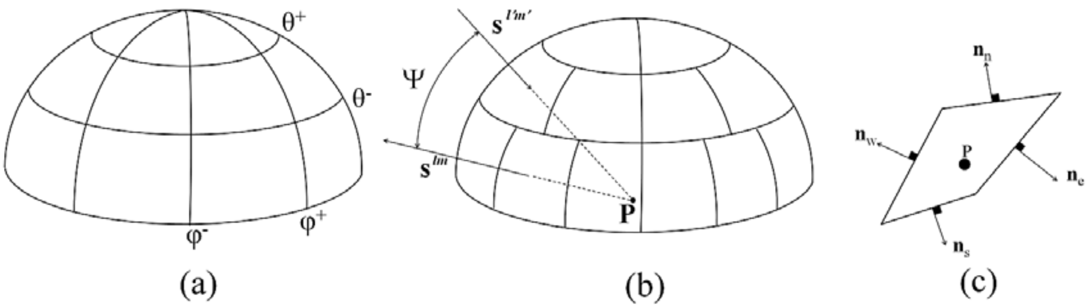

Fig 1: (a) Angular discretization for popular FVM, (b) angular discretization for FT_6 FVM, (c) an arbitrary control volume with its representative node and surface normal vectors.

The formulation of terms associated with the CLAM scheme can be found in [17, 18] and is not repeated here. The Eq. (4) is solved with an iterative approach with TDMA algorithm. The iteration stops when the following condition is satisfied:

$$\max\left|\frac{I_P^l - I_{P,old}^l}{I_{P,old}^l}\right| \le 10^{-8} \tag{5}$$

If the analytical expression for scattering phase function ($\Phi(\mathbf{s},\mathbf{s}')$) exists, the average scattering phase function in Eq. (2) can be obtained by the following relation:

$$\overline{\Phi}(\mathbf{s},\mathbf{s}') = \frac{\int_{\Delta\Omega^l}\int_{\Delta\Omega^{l'}} \Phi(\mathbf{s},\mathbf{s}')d\Omega' d\Omega}{\Delta\Omega^l} \tag{6}$$

When the integration is not feasible or $\Phi(\mathbf{s},\mathbf{s}')$ is an unknown function but its value for different **s** and **s′** can be obtained, its average can be estimated by the following formula:

$$\overline{\Phi}(\mathbf{s},\mathbf{s}') = \frac{\sum_{l_s=1}^{L_s}\sum_{l_{s'}=1}^{L_{s'}} \Phi^{l_s,l_{s'}} \Delta\Omega^{l_s} \Delta\Omega^{l_{s'}}}{\Delta\Omega^l} \tag{7}$$

For particulate media of this study, the analytical expression for scattering phase function does not exist and therefore Eq. (7) must be used. Scattering phase function in any combination of **s** and **s′** is obtained by applying Mie theory. The details of complicated Mie theory are beyond the scope of this work. We have used the same formulations and approximation method as explained in [2].

3. Results and discussion

The geometry of computational domain and its 15×15 non-orthogonal curvilinear grid system are displayed in Figs. 2a and 2b, respectively. Wall number 5 (the quadrant) is hot with $E_{b,ref}$=1 W/m^2. Other walls and the medium are cold at 0K. Walls number 1 and 4 are diffuse reflectors (ε_w=0). Walls number 2 and 3 are black. The parameters investigated are the dimensionless direction-averaged intensity (G) of the symmetry line *b-b* (Fig. 2a) and the dimensionless heat flux (q) on the right wall (*wall 2*). It is found that further refinement of the grid system does not change the results. The grid independency check is shown in Fig. 2c. It presents the dimensionless G along the line *b-b* when the domain contains carbon particles at x_p=2 and N_T=10^5 (particles/cm^3).

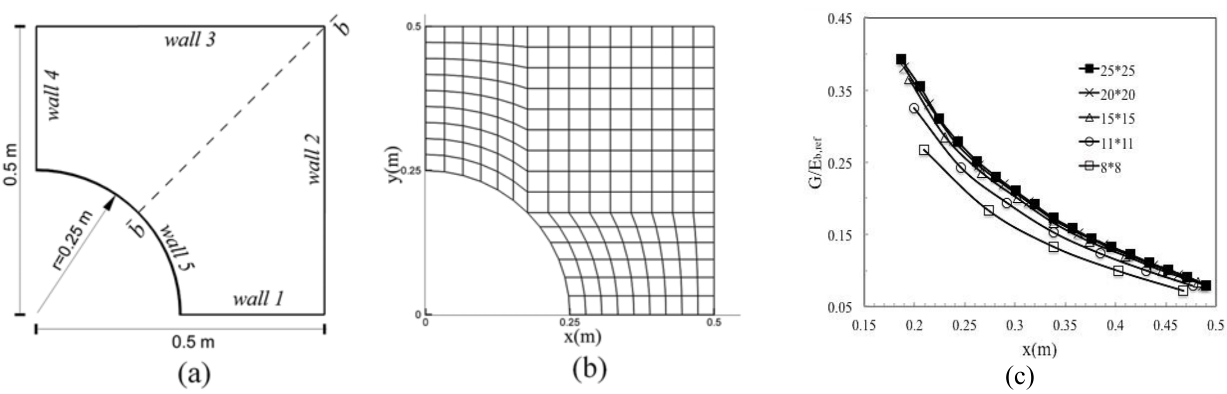

Fig 2: (a) Geometry, (b) grid pattern of the computational domain, (c) grid independency check.

The effect of different materials of Table 1 is studied. The radiative heat transfer in medium with ash particles is more intense as can be seen in Fig. 3a. The difference in the values of radiative flux of Fig. 3a is mainly attributed to the values of β and ω. Besides the fact that the radiative intensity travels with less changes in a media with lower extinction coefficient, the value of single scattering albedo has a significant impact on radiative transfer according to Eqs. (1-2). In a cold medium, the first term on the right of Eq. (2) tends to zero and the source term reduces. Therefore, the ratio of σ_s to β becomes important and higher ω leads to higher radiative intensity. As a result, the heat flux in a medium such as ash with lower value of β and higher value of ω must be stronger. At the bottom points of the right wall, the distance to the hot wall (the quadrant) is lowest and one may expect the highest heat flux. But due to closeness to a cold wall (*wall 1* in Fig. 2a) the peak of heat flux does not occur there. By going up along the right wall, the effect of the cold wall reduces and the maximum heat flux occur approximately at y=0.1 m. Hereafter, a decreasing trend is seen due to increase in the distance from the quadrant which is the source of radiation. In Fig. 3b the dimensionless G along the centerline is shown for various media. It is observed that G decreases by going away from the hot wall.

Table 1: Media with different complex indices of refraction [10]

Particle material	*n*	*k*
Carbon	2.20	1.12
Anthracite	2.05	0.540
Bituminous	1.85	0.220
Lignite	1.70	0.066
Ash	1.50	0.020

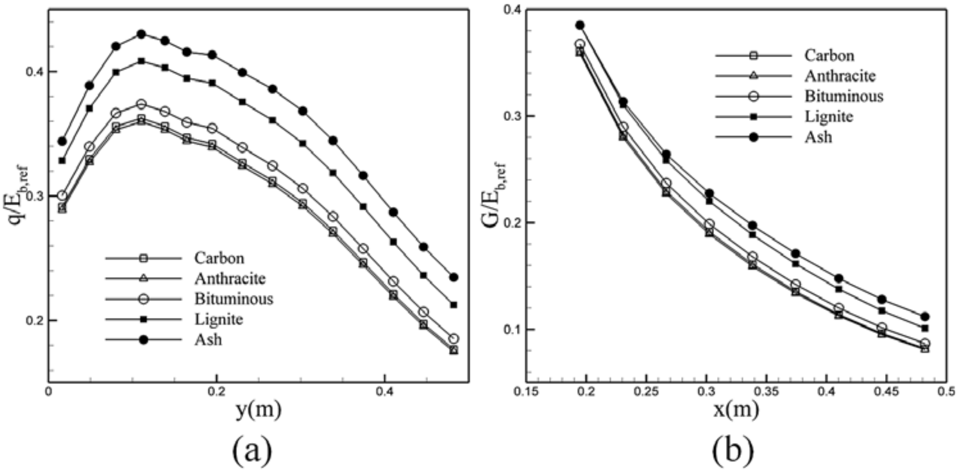

Fig 3: Results for different types media of Table 1 at x_p=2 and N_T=10^5 (particles/cm^3) (a) dimensionless heat flux on the bottom wall, (b) dimensionless direction-averaged intensity along line *b-b*.

The effects of particle size x_p and density N_T are also studied. In this case, the radiative equilibrium condition is applied to govern the temperature field inside the enclosure. The results are exhibited in Figs. 4 and 5. According to Mie theory, if the particles in the medium have the same size, the scattering and extinction coefficient of the particles can be expressed as:

$$\sigma_{s,\lambda} = \pi a_p^2 N_T Q_{sca} \qquad \beta_\lambda = \pi a_p^2 N_T Q_{ext} \tag{8}$$

Based on Eq. (8), there is a linear relationship between β and σ_s with N_T. Therefore, by changing N_T, the extinction coefficient changes and the single scattering albedo remains constant. On the other hand, the higher contribution of medium in radiative heat transfer takes place when the extinction coefficient goes up. With the radiative equilibrium condition, some of the energy that a beam carries is consumed to warm up the medium. Also, the effect of boundary temperature becomes more significant. Therefore, less energy reaches the cold walls and lower values of heat flux are seen for higher values of N_T as can be seen in Fig. 5a. Conversely, as seen in Fig. 5b, at higher values of N_T the temperature gap inside the domain becomes more pronounced because the heat from the hot boundary is extenuated by the medium due to higher value of β. According to Eq. (1), when the medium is optically thicker, i.e. has higher β, the rate of decrease in the intensity becomes larger as the first term on the right hand side of Eq. (1) increases. This explains the reason for higher temperature gap in the medium with higher values of N_T.

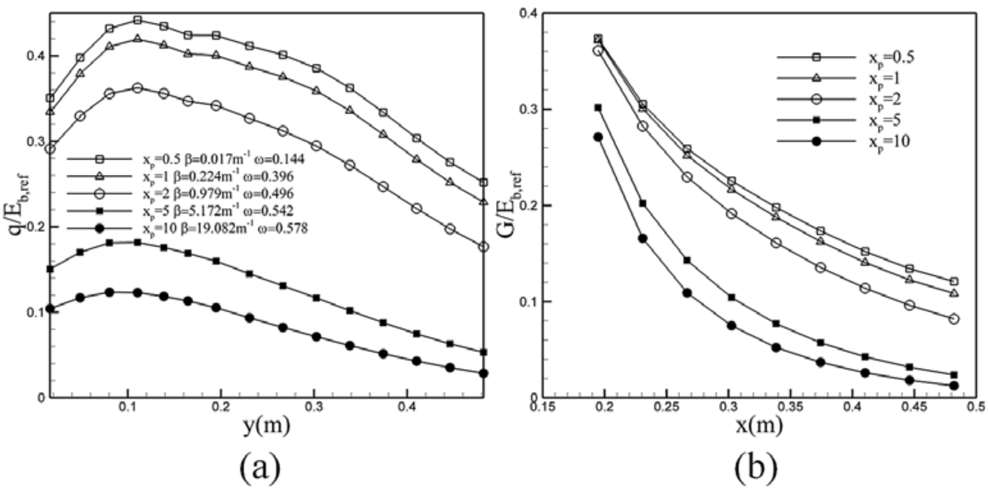

Fig 4: Results for a medium of carbon particles at N_T=10^5 (particles/cm^3) (a) dimensionless heat flux on the bottom wall and (b) dimensionless G along line *b-b*.

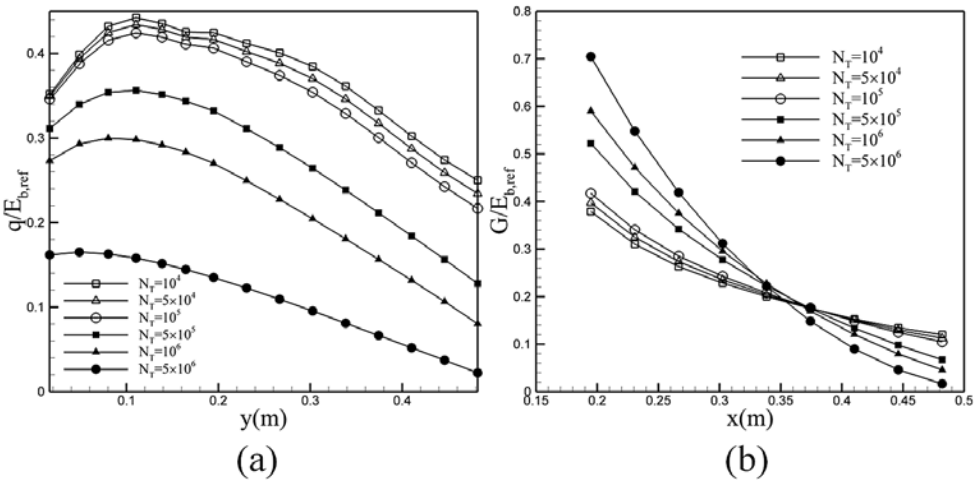

Fig 5: Results for a medium of carbon particles at x_p=2 (a) dimensionless heat flux on the bottom wall (b) dimensionless G along line *b-b*.

4. Conclusions

In this work the radiative heat transfer problem in particulate media is solved numerically. The computational domain is an irregular enclosure. Particles are considered as spheres with their radii varying between 250 nanometers and 5 micrometers. The effects of particle size and particle density in the media are investigated. It is found that:

- Radiative heat flux on the cold surface is higher for forward scattering media. Also, the range of *G* is wider for backward scattering;
- The radiative flux and integrated intensity are higher for media of fly ash particles;

- The effect of cold walls is important in predicted values of heat flux;
- For a denser media, the radiative flux is lower but the values of the directionally integrated intensity cover a wider range due to more radiative heat transfer.

References

[1] Trivic DN, O'Brien TJ, Amon CH. Modeling the radiation of anisotropically scattering media by coupling Mie theory with finite volume method. International journal of heat and mass transfer. 2004; 47(26):5765-80.
[2] Moghadam EK, Isfahani RN, Azimi A. Numerical Investigation of the Transient Radiative Heat Transfer inside a Hexagonal Furnace Filled with Particulate Medium. Am. J. Mech. Eng. 2016; 4(2):42-9.
[3] Fiveland WA. Three-dimensional radiative heat-transfer solutions by the discrete-ordinates method. Journal of Thermophysics and Heat Transfer. 1988; 2(4):309-16.
[4] Raithby GD, Chui EH. A finite-volume method for predicting a radiant heat transfer in enclosures with participating media. Journal of Heat Transfer. 1990; 112(2):415-23.
[5] Chai JC, Lee HS, Patankar SV. Finite volume method for radiation heat transfer. Journal of thermophysics and heat transfer. 1994; 8(3):419-25.
[6] Kisselev VB, Roberti L, Perona G. An application of the finite element method to the solution of the radiative transfer equation. Journal of Quantitative Spectroscopy and Radiative Transfer. 1994; 51(4):603-14.
[7] Liu LH. Finite element simulation of radiative heat transfer in absorbing and scattering media. Journal of thermophysics and heat transfer. 2004; 18(4):555-7.
[8] Howell JR, Perlmutter M. Monte Carlo solution of thermal transfer through radiant media between gray walls. Journal of heat transfer. 1964; 86(1):116-22.
[9] Hottel HC, Cohen ES. Radiant heat exchange in a gas filled enclosure: Allowance for nonuniformity of gas temperature. AIChE Journal. 1958; 4(1):3-14.
[10]Modest MF. Radiative heat transfer. Academic press; 2013.
[11]Howell JR, Menguc MP, Siegel R. Thermal radiation heat transfer. CRC press; 2010.
[12]Chen X, Xia XL, Sun C, Yan XW. Transient thermal analysis of the coupled radiative and convective heat transfer in a porous filled tube exchanger at high temperatures. International Journal of Heat and Mass Transfer. 2017; 108:2472-80.
[13]Sun HF, Sun FX, Xia XL. A line-by-line hybrid unstructured finite volume/Monte Carlo method for radiation transfer in 3D non-gray medium. Journal of Quantitative Spectroscopy and Radiative Transfer. 2018; 205:135-46.
[14]Moghadassian B, Kowsary F, Mosavati M. The radiative boundary design of a hexagonal furnace filled with gray and nongray participating gases. Journal of Thermal Science and Engineering Applications. 2013; 5(3):031005.
[15]Jo SM, Kim JW, Kwon OJ. A narrow-band k-distribution model with single mixture gas assumption for radiative flows. Infrared Physics & Technology. 2018; 91:27-36.
[16]Moghadassian B, Kowsary F. Inverse boundary design problem of natural convection–radiation in a square enclosure. International Journal of Thermal Sciences. 2014; 75:116-26.
[17]Kim SH, Huh KY. A new angular discretization scheme of the finite volume method for 3-D radiative heat transfer in absorbing, emitting and anisotropically scattering media. International Journal of Heat and Mass Transfer. 2000; 43(7):1233-42.
[18]Kamel G, Naceur BM, Rachid M, Rachid S. Formulation and testing of the FTn finite volume method for radiation in 3-D complex inhomogeneous participating media. Journal of Quantitative Spectroscopy and Radiative Transfer. 2006; 98(3):425-45.